

Contrastive Neighborhood Alignment

Pengkai Zhu*
Amazon/AWS AI

Zhaowei Cai*
Amazon/AWS AI

Yuanjun Xiong*
Amazon/AWS AI

Zhuowen Tu*
Amazon/AWS AI

Luis Goncalves
Amazon/AWS AI

Vijay Mahadevan
Amazon/AWS AI

Stefano Soatto
Amazon/AWS AI

Abstract

We present Contrastive Neighborhood Alignment (CNA), a manifold learning approach to maintain the topology of learned features whereby data points that are mapped to nearby representations by the source (teacher) model are also mapped to neighbors by the target (student) model. The target model aims to mimic the local structure of the source’s representation space using a contrastive loss. CNA is an unsupervised learning algorithm that does not require ground-truth labels for the individual samples. CNA is illustrated in three scenarios: manifold learning, where the model maintains the local topology of the original data in a dimension-reduced space; model distillation, where a small student model is trained to mimic a larger teacher; and legacy model update, where an older model is replaced by a more powerful one. Experiments show that CNA is able to capture the manifold in a high-dimensional space and improves performance compared to the competing methods in their domains.

1. Introduction

In this paper, we present a new algorithm, Contrastive Neighborhood Alignment (CNA), that preserves the local topology of learned features between source and target models by mapping neighbors in one space (source) to neighbors also in the target (student) space. CNA overcomes the optimization challenge in the formulation of traditional manifold learning methods for large-scale computing by designing a contrastive loss that can be trained effectively to preserve the local topology of the feature space. The model learned through CNA is inductive and hence can generalize to novel data. CNA is an unsupervised approach and requires no ground-truth labels. Fig. 1 illustrates the local topology preservation by CNA, that the neighbors (x_5, x_7, x_8) of a sample x_1 (Fig. 1 left) in the source space is well-preserved in the target model space trained by

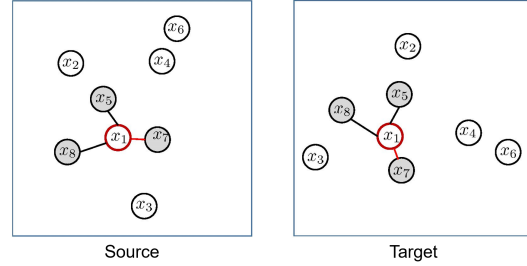


Figure 1. The local topology of feature space in source (left) and target (right) models. CNA preserves the local structure between models, such that the neighbors (x_5, x_7, x_8 for x_1) from the source model stay the same in the target model.

CNA(Fig. 1 right).

CNA does not impose constraints on source models and it can be adopted to performing student-teacher learning for tasks such as knowledge distillation (KD) [16] and reducing model regression in model updating [51], beyond the standard manifold learning tasks [9, 34, 42]. Conventional knowledge distillation and student-teacher (S-T) learning [1, 7, 16, 47] approaches primarily follow the design principle of matching features or classification distributions between the teacher and student models [47]. Despite the effectiveness of the feature/distribution matching criterion, S-T learning methods are not without limitations. Typically, student-teacher training tries to force the student to mimic the input-output behavior of the teacher, but the regularization term (model bias) often results in a direct conflict with the cross-entropy (CE) loss, i.e., KL-divergence/logit-matching vs. softmax. This has two problems. First, the criterion trades off error rate minimization. Second, the criterion is too rigid in that it mimics the teacher’s predictions without the awareness of the data manifold. In contrast, CNA tackles the student-teacher learning problem by modeling the knowledge in the models using the local structures in their feature space, which is distinct from the existing methods in model distillation [16].

CNA is a new inductive principle: instead of mimicking the input-output behavior, it transfers the local neighbor-

*equal contribution

hood structure. Neighbors remain neighbors, when transferring from the source to the target, regardless of the label. This has two distinct advantages: first, it does not require ground truth labels. Second, it allows more flexibility to deviate from the inference of the source model when it is mistaken. In CNA, we impose that samples are neighbors in the source (teacher) representation space remain neighbors in the target (student) representation space. This alignment of local neighborhoods is achieved by adding to the cross-entropy loss a contrastive term that is in the same form (softmax function) as the cross-entropy term, making the optimization well conditioned; as both the cross-entropy and the contrastive loss are in similar unit spaces (normalized softmax function), balancing the two terms becomes relatively easy. The contributions of our work are listed below:

- We propose a new method for manifold learning that maintains the local neighborhood in inductive models.
- We introduce an instance-level contrastive loss for preserving the neighborhood structures that is different from how contrastive loss is motivated and implemented previously [15, 30, 49].
- We propose to use a new loss function in Student-Teacher training, which is distinct from the existing methods in this field.

The effectiveness of CNA is demonstrated on three tasks, 1) dimensionality reduction for manifold learning [45], 2) model distillation [16], and 3) model update regression minimization [51]. CNA is capable of capturing the manifold from the source space and can be applied to various downstream tasks in knowledge distillation.

2. Related work

Manifold/metric learning: Preserving local neighborhood structure is a popular direction in machine learning that has been explored in both metric learning [8, 17, 26, 52] and manifold learning [34]. Standard manifold learning approaches perform dimensionality reduction by mapping the feature representation from the original space to the new one [45]. They attempt to maintain the local structure through the reconstruction by the convex combination of same neighbors [9, 34], by retaining the neighborhood distances while unfolding the manifold [48], or by preserving pairwise geodesic distances between all data points [42]. These manifold learning methods learn the manifold transductively, which limits their deployments in modern deep networks. In contrast, Our CNA adopts an instance-level contrastive loss that attempts to preserve the manifold structure of feature space in an inductive model, which is significantly different from these works. Additionally, CNA can be combined with classification loss (e.g. a cross-entropy loss) to create classifiers when training deep models.

Contrastive learning and self-supervised learning: Contrastive learning [12] is used for either supervised [20, 37, 41] or unsupervised [6, 14, 49] representation learning. It has recently become popular in self-supervised learning through the instance discrimination pretext task [49]. Contrastive representation distillation (CRD) [43] extends the idea of contrastive learning to the teacher-student training case. Though not directly minimizing a certain distance function, CRD still needs to calculate the distance between student’s feature vectors and that of the teacher. CNA uses the contrastive loss form in teacher student training but does not measure the “cross model distance”. It only concerns the local structures within the models’ feature spaces. The supervised contrastive learning method [20] is also different from CNA since we focus on preserving the local neighborhoods between models as opposed to using class labels to learn visual representation.

Model distillation: There has been a significant amount of work to study how knowledge can be shared between multiple models. Model distillation [16, 47] transfers knowledge from a larger, more powerful teacher model to a smaller student model by matching their output/representation. CNA does not rely on matching outputs [16, 51] or reusing the old models’ parameters [38]. Instead, knowledge is shared between models through the information encoded in the neighborhood structure of a model’s feature space.

Regression minimization for model upgrading: The presence of new errors that were not manifest when using the old model (negative flips) can cause a perceived reduction of performance by users, referred to in the industry as “regression.” Although progress in the design of the architecture of backbone models [15, 18, 19, 39, 40, 46, 50], new optimization and regularization schemes [4, 10, 24], and the availability of new datasets [3, 22, 25, 28, 33, 35] have driven a fast-paced reduction of the average error rate (AER) of image classifiers, regression is still a major obstacle to the deployment of improved models. Even a modest number of negative flips can nullify the benefit of a large decrease in AER. Overall, the problem of reducing the negative flip rate (NFR), along with the average error rate (AER), has been referred to as Positive-Congruent Training, or PC-Training [51]. Minimizing model regression during model upgrading is an emerging problem that is of great practical importance [51]. In [51], NFR is proposed as the metric to measure regression in classification model updates and an approach based on focal distillation, a variant of model distillation [16], is proposed to reduce regression. Our work addresses the same problem through contrastive neighbor alignment instead of relying on model distillation.

3. Contrastive Neighborhood Alignment

Given a possibly pretrained source model S and a dataset $\mathcal{D} = \{x_i\}$, it is a common task to transfer information

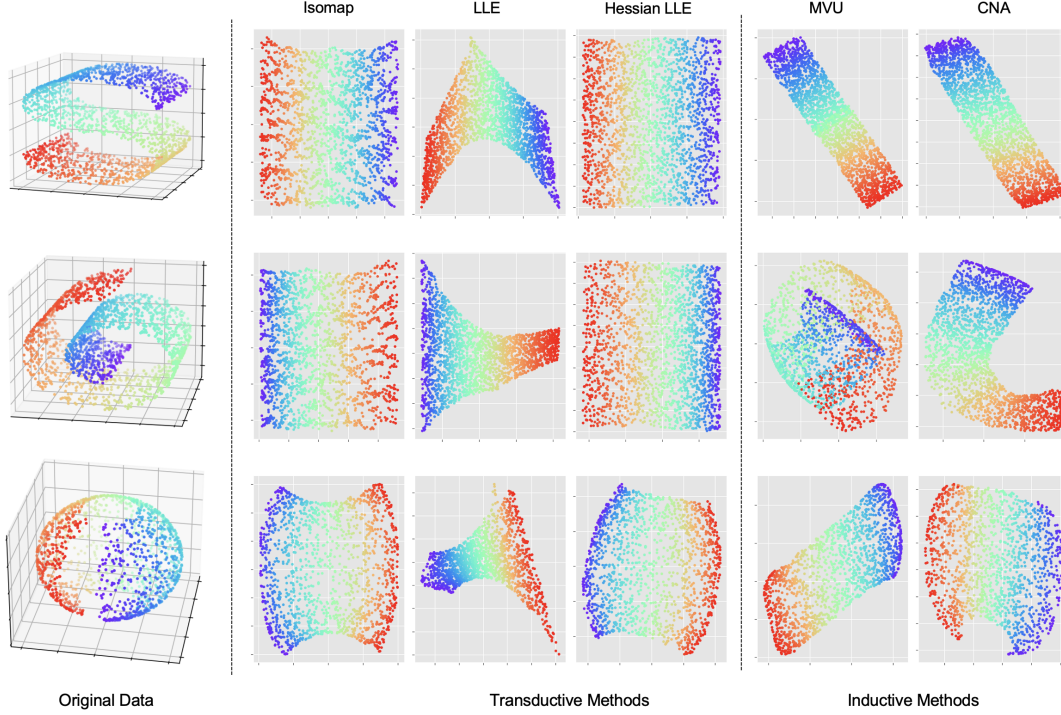


Figure 2. Qualitative results of manifold learning on synthetic datasets. Rows(top to bottom): S-curve, Swiss Roll, Sphere. Columns(left to right): original 3D data points, transductive methods (Isomap [42], LLE [34], Hessian LLE [9]), inductive methods (MVU [48], CNA).

from the source model S to a newly trained target model T . Let $f_S(\cdot)$ and $f_T(\cdot)$ denote the feature representation of the source and target model, respectively. The two models could have different architectures or different feature dimensions. For example, in manifold learning [45], the high-dimensional source feature space is cast to a target space in which the low-dim manifold is unveiled. In model distillation, knowledge is shared between models by minimizing the sample-wise pseudo-distance between the two models' classification posterior probabilities. In this work, we propose CNA, a contrastive loss that transfers information between models by preserving of the local structures of the source model feature space in that of the target. An illustration of this idea is shown in Fig. 1. Below, we detail the derivation of the CNA loss function and its applications in model distillation/update tasks.

3.1. Preserving Local Structure

The idea of replicating the local structure in a new feature space has been explored in the manifold learning literature [45]. For example, Isomap [42] preserves pairwise geodesic (or curvilinear) distances between samples. The geodesic distances are computed by constructing a neighborhood graph in which every sample x_i is connected with its top- K nearest neighbors. Locally linear embedding (LLE) [34] studied the local structure in the non-linear feature space. It has shown that by embedding high-dimensional feature vectors in their local neighborhoods,

we can obtain effective low-dimensional embedding of the data points. LLE assumes each data point and its neighbors lie on a locally linear patch in the source space, and characterizes the local structure by a linear reconstruction using the neighbors:

$$\epsilon(W) = \sum_i \|f_S(x_i) - \sum_j W_{i,j} f_S(x_j)\|_2^2 \quad (1)$$

where $f_S(x_i)$ is the feature representation of x_i in the source space, ϵ is the reconstruction error and W is the coefficient matrix. $W_{i,j}$ is enforced to 0 if x_j is not one of the top- K neighbors of x_i and $\sum_j W_{i,j} = 1$. The solution $W^* = \arg \min \epsilon(W)$ is then used to obtain the target representation by minimizing the reconstruction error in the target space. Maximum Variance Unfolding (MVU) [48] is another work that focuses on retaining pairwise distances in a neighborhood graph. It maximizes the sum of distances between all data points in the target space:

$$\max \sum_{i,j} d(f_T(x_i), f_T(x_j)), \quad (2)$$

under the constraint that the distances between the neighbors are preserved: $d(f_T^{(i)}, f_T^{(j)}) = d(f_S^{(i)}, f_S^{(j)})$ if x_j is one of the top- K neighbors of x_i . Here $d(\cdot, \cdot)$ is the ℓ_2 distance.

However, these manifold learning methods are difficult to be employed in modern deep learning frameworks. They often need to store a local structure graph for the entire

dataset, which occupies a lot of memory. Inferring the representation for each data point is also not viable when the dataset is large. The features are assumed to live in the same metric space defined by the ℓ_2 distance function, which is often not the case for highly non-linear deep neural networks. The generalization to novel data is also difficult due to the transductive nature of these methods (see discussions in Sec. 3.2).

Inspired by these approaches, and to remedy these issues, CNA is proposed to preserve the local structure in the target model’s feature space by enforcing the same neighbors from the source space.

3.2. Contrastive Neighborhood Alignment Loss

We hypothesize that the knowledge can be shared between two models when the nearest neighbors of x_i in the source model’s feature space are still its nearest neighbors in the target model’s feature space. For simplicity, we can set $K = 1$ in Eq. (1), resulting in each sample’s feature $f_T(x_i)$ being represented only by its nearest neighbor $f_T(x_{i^*})$ in the feature space, with $W_{ii^*} = 1$. Then the learning objective can make the target model maintain the local structure encoded by W in its own feature space. By resorting to instance-based contrastive loss, we propose the contrastive neighborhood alignment (CNA) loss that achieves the goal of matching the same neighbors in an easy to optimize manner.

Specifically, for each sample x_i in a batch of M samples, we locate its nearest neighbor $\aleph(x_i)$ in the feature space of the source model:

$$\aleph(x_i) = x_{i^*}, \quad (3)$$

where

$$i^* = \arg \max_{j=1, \dots, M, j \neq i} \frac{f_S(x_i) \cdot f_S(x_j)}{\|f_S(x_i)\|_2 \cdot \|f_S(x_j)\|_2}, \quad (4)$$

where $f_S(\cdot)$ is the feature representation of the source model and $\|\cdot\|_2$ is the ℓ_2 norm of the feature. The nearest neighborhood is the indicator we use for the model local topology. And the contrastive neighborhood alignment loss is designed to encourage the target model to maintain the same local neighborhood structure,

$$\ell_{\text{CNA}}(x_i) = -\log \frac{\exp[f_T(x_i) \cdot f_T(\aleph(x_i))/\tau]}{\sum_{j \neq i}^M \exp(f_T(x_i) \cdot f_T(x_j)/\tau)}, \quad (5)$$

where τ is the temperature, and $f_T(\cdot)$ the target feature extractor and its output is assumed normalized. Instead of directly minimizing the distance between neighbors, in Eq. (5), the neighbor pairs defined by the source model are pulled together but the non-neighbor pairs will be pushed away during the target model training. In this way, the local structure is preserved, and the knowledge encoded in the structure is transferred to the new model.

The contrastive loss has the same softmax form as the cross-entropy loss, and this helps when both losses need to be jointly optimized. More importantly, there is no longer a direct requirement to match the source and target outputs. This relaxation enables the CNA to be applicable even when the target model is trained with different loss functions or has different feature dimensions.

While the CNA loss of Eq. (5) only considers the nearest neighbor, it can be easily generalized to top- K nearest neighbors,

$$\ell_{\text{CNA}}^K(x_i) = \frac{1}{K} \sum_{\tilde{x} \in \aleph^K(x_i)} -\log \frac{\exp[f_T(x_i) \cdot f_T(\tilde{x})/\tau]}{\sum_{j \neq i}^M \exp(f_T(x_i) \cdot f_T(x_j)/\tau)}, \quad (6)$$

where $\aleph^K(x_i)$ is the top- K nearest neighbors of sample x_i . This formulation simply averages the CNA losses of multiple neighbors.

Transductive vs. Inductive: Traditional manifold learning methods are transductive as they infer the target representation for each data point directly by optimizing the objective. It is advantageous in capturing the manifold of training data since the projection is not limited by any function. But they are hard to generalize to novel data as it requires modification of the original graph. Our CNA is fundamentally different as we learn an inductive target model by making the new model mimic the local structure of the source representation space. In experiments, we show that CNA can also be used to learn an inductive model, and it is non-trivial to adapt the transductive method into an inductive model.

3.3. Model Distillation/Update

By distilling the knowledge of the source (teacher) model to the target (student) model, the target model can achieve higher accuracy [16] or maintain consistency when the model is updated [51]. There are various definitions of knowledge which leads to different approaches to transfer it. The objective can be to minimize the sample-wise feature distance between two models with respect to a feature distance function, usually ℓ_2 -distance [36]. Recent works also proposed to use the contrastive loss [20] instead of minimizing absolute distance. Our CNA can also be used in these tasks, by carrying the knowledge of the teacher model to the student model by preserving the local structure of the feature space.

Let us consider a classification problem. Let $y_i \in \{1, 2, \dots, C\}$ denote the class label for each data sample x_i . $h(\cdot, \cdot)$ is the classifier following the feature extractor $f(\cdot)$ to predict the class label, $\hat{y} = \arg \max_y h(f(x), y)$. In order to learn the full target classification model $\{f_T, h_T\}$ capable of preserving the local topology of the teacher model, the final objective is defined as the weighted sum of the standard

cross-entropy loss and the CNA loss:

$$\mathcal{L}_{\text{CNA}} = \frac{1}{M} \sum_i^M [\ell_{\text{CE}}(x_i, y_i) + \lambda \ell_{\text{CNA}}(x_i)], \quad (7)$$

where λ is the trade-off coefficient, and ℓ_{CE} is the cross-entropy loss,

$$\ell_{\text{CE}}(x_i, y_i) = -\log \frac{\exp(h_T(f(x_i), y_i))}{\sum_c \exp(h_T(f(x_i), y_c))}, \quad (8)$$

where $y_c = 1, 2, \dots, C$ refers to each class in the datasets. Note that the prediction of the source model $h_S(\cdot, \cdot)$ is not present in the loss function Eq. (7), unlike the distillation term in knowledge distillation methods [16]. Thus, the two terms in Eq. (7) stay congruous even if the source model makes mistakes. As stated before, another major advantage of our proposed CNA loss is the formulation consistency between the two terms, and balancing the two terms in the loss function is relatively easy.

4. Experiments

We first evaluate the performance of the proposed CNA method on the unsupervised dimensionality reduction task and compare to other manifold learning techniques. CNA is then evaluated on two real-world application tasks: model distillation (from a large to small model) and model update (from a small to a large model).

4.1. Manifold Learning/Dimensionality Reduction

In a dimensionality reduction task, the goal is to learn a low-dimensional embedding that captures the manifold in the high-dim data space and favors downstream classifications. The source model $f_S(\cdot)$ reduces to an identity function and the target model $f_T(\cdot)$ is a projector that maps data to a lower dimensional space. We perform the experiments on synthetic datasets and natural datasets. On synthetic datasets, we show qualitative results to demonstrate that CNA is capable of discovering the manifold in a low-dimensional space. On natural datasets, we report quantitative results to measure the quality of the learned embeddings. In this task, CNA is employed in an unsupervised fashion where the cross-entropy loss in Eq. (7) is absent.

Baselines: We compare to three transductive manifold learning methods: Isomap [42], LLE [34] and Hessian LLE [9]. We use CNA to learn an inductive function through neural networks on both synthetic and real-world data. We also propose an inductive baseline trained by a modified MVU [48] objective. Specifically, this baseline uses the

Table 1. Quantitative results in % on real-world data. Local-err: local error on training set; 5-NN Acc: generalization accuracy on test set using a 5-NN classifier trained on the low-dimensional space. The inputs are projected to 40-dim space. *:Hessian LLE uses a 10-dim space due to the constraint on available neighbors [48]. †: CNA can reduce training error but with lower test accuracy.

Methods	Tr./Ind.	MNIST		CIFAR10	
		Local-err	5-NN Acc	Local-err	5-NN Acc
Isomap	Tr.	9.3	91.2	4.2	88.7
LLE	Tr.	10.0	91.3	3.4	88.9
Hessian*	Tr.	15.4	88.2	4.1	88.9
MVU	Ind.	34.1	72.3	3.9	88.2
CNA	Ind. (ours)	8.7	92.3	3.9	89.3
CNA†	Ind. (ours)	-	-	3.2	88.7

same inductive network as CNA and is trained by:

$$\begin{aligned} \ell_{\text{MVU}} = \frac{1}{M} \sum_i^M \left\{ \frac{1}{K} \sum_{j: x_j \in \mathbb{N}^K(x_i)} [d(f_S(x_i), f_S(x_j)) \right. \\ \left. - d(f_T(x_i), f_T(x_j))]^2 - \gamma \sum_{\substack{j: j \neq i \\ x_j \notin \mathbb{N}^K(x_i)}} d(f_T(x_i), f_T(x_j)) \right\} \end{aligned} \quad (9)$$

where γ is a balance weight. Basically, this loss function will push non-neighbor data points far away while keeping the distance between neighbors in the target space. During the experiments, we found a small γ is necessary (1e-6 e.g.) to avoid trivial solutions where every sample is isolated.

Implementations: For Isomap, LLE and Hessian LLE, the only free parameter is the number of neighbors K . We set it to 10 on synthetic data and sweep over [5, 10, 50, 100, 200] on real-world datasets. For MVU and CNA, we use a 3-layer multi-layer perceptron (MLP) with Tanh activation function as the inductive projection model. All networks are trained by Adam optimizer [21] with batch size 256. We fine-tuned the learning rate, number of neighbors K , temperature τ and γ in Eq. (9) on a held-out validation set.

4.1.1 Synthetic Data

We performed experiments on three synthetic datasets: S-Curve, Swiss Roll, and Sphere. Data points lie on a two-dimensional manifold in the original 3D space. The plots of the datasets are shown in the left column of Fig. 2. All datasets contain 2000 samples. The learning is considered good if the manifold is unfolded and the local structure is retained in the projected 2D space. In the experiments, the MVU and CNA networks have an intermediate layer with 5 nodes and hence 60 total parameters. All networks are trained for 2000 epochs. We visualize the learned manifolds for all the methods in Fig. 2.

The results show that the proposed CNA is capable of unfolding the manifold on all three synthetic datasets. The data points with similar colors stay neighbors in the projected space. Hence the local topology is well maintained. Transductive manifold learning methods can also unfold the manifold. However, on Swiss Roll dataset, the inductive MVU method fails to retrain the manifold even though we extensively fine-tuned the parameters. This indicates the non-triviality of achieving manifold learning using inductive networks. Notice that although the reconstructed manifolds of CNA for Swiss Roll have a non-linear warping, they are not considered poor as the local structure of the two manifolds is identical to that of Isomap and Hessian LLE. Moreover, compared to transductive methods, CNA can learn the manifold using an inductive function with a handful parameters.

4.1.2 Real-world Data

We conducted experiments on two real-world datasets: MNIST [27] and CIFAR10 [23]. On MNIST we use the original data (784-dim) as source space, and on CIFAR10 we use the perceptual features (512-dim) of a pretrained ResNet18 model as the source data. For computational efficiency, we randomly select 4000 samples as training data and 1000 samples as test data. The intermediate layer of the MVU and CNA networks has 512 nodes. The networks are trained by 1000 epochs. The data is projected to a 40-dim space except for Hessian LLE because the number of neighbors required is proportional to the square of dimension [48]. The baseline transductive methods are more competitive, not less, as we found $\text{dim}=40$ works the best for most transductive methods.

Metrics: We evaluated two metrics: local error and 5-NN generalization accuracy [45]. Local error is the rate of samples in the training set of which the nearest neighbor is not from the same class. It measures whether the neighbors are maintained in the low-dimensional space. 5-NN generalization accuracy is defined as the accuracy on the test set using a 5-nearest neighbor classifier trained on the projected space. It reflects the quality of the learned data representation regarding the downstream classification task.

The quantitative results on real-world datasets are tabulated in Tab. 1. The proposed CNA method shows competitive results across the board. It outperforms all other methods on MNIST and achieves the best 5-NN accuracy on CIFAR10. CNA has higher training local error on CIFAR10. We argue that CNA focuses on broader local topology rather than the nearest neighbor, in order to achieve better generalization when the data is more complex. It can reach lower training error with a sacrifice on the test accuracy (see CNA † in Tab. 1). Based on these observations, we conclude that CNA can effectively conduct manifold learn-

Table 2. The model distillation results (top-1 accuracy in %) on CIFAR100. * denoted results run by us. The other results of the competitors are from [43].

Teacher (Source)	ResNet56	ResNet110	ResNet110	ResNet32x4	ResNet32x4	ResNet32x4
Student (Target)	ResNet20	ResNet20	ResNet32	ResNet8x4	ShuffleNetV1	ShuffleNetV2
Teacher (Source)	72.90	74.25	74.25	79.67	79.67	79.67
Student (Target)	69.96	69.96	71.26	72.68	70.98	71.76
KD* [16]	71.82	71.33	73.81	73.55	75.05	75.54
SP [44]	69.67	70.04	72.69	72.94	73.48	74.56
CC [32]	69.63	69.48	71.48	72.97	71.14	71.29
VID [2]	70.38	70.16	72.61	73.09	73.38	73.40
RKD [31]	69.61	69.25	71.82	71.90	72.28	73.21
LFA*	71.85	71.75	73.79	72.41	75.07	75.43
CNA (ours)	71.96	71.30	73.63	74.66	75.20	75.44

Table 3. The model distillation results (top-1/top-5 accuracy in %) on ImageNet.

	ResNet34	ResNet18 KD [16]	CRD [43]	LFA	CNA (ours)
top-1	73.31	69.76	71.33	71.17	71.41
top-5	91.42	89.08	90.35	90.13	90.36

	ResNet50	ResNet18 KD [16]	CRD [43]	LFA	CNA
top-1	76.13	69.76	71.25	-	70.80
top-5	93.55	89.08	90.53	-	90.13

ing with an inductive function.

4.2. Real-World Applications

We evaluated the proposed CNA method on two real-world tasks: model distillation and model update. In both tasks, information from one model is expected to transfer to another model, and our CNA method can be applied by considering the teacher (old) model as source and the student (new) model as target in model distillation (update). ImageNet [35] and CIFAR100 [23] are the two major datasets used for evaluation. The used network architectures are the standard ResNet variants [15] on ImageNet, and ResNet [15] and ShuffleNet [29, 53] on CIFAR100 following [43].

Training Details: For CIFAR100 (ImageNet), the base initial learning rate was 0.2 (0.1) for batch size of 256, linear scaling [11] was used for other batch sizes, and cosine learning rate decay schedule was adopted. Weight decay was set as 0.0001 for all ImageNet experiments, but it is sensitive and we searched the best one from $\{0.0001, 0.0002, 0.0005\}$ for CIFAR100. SGD was used for optimization in all experiments. For CNA, we set $\lambda = 1.0$ in Eq. (7) and temperature $\tau = 0.01$ in Eq. (5) for all experiments. Each experiment of CIFAR100 (ImageNet) is conducted on 4 (8) V100 GPUs for about 1 (15) hour(s). The results were averaged on 5 runs for all CIFAR100 experiments. More details will be introduced in the following section.

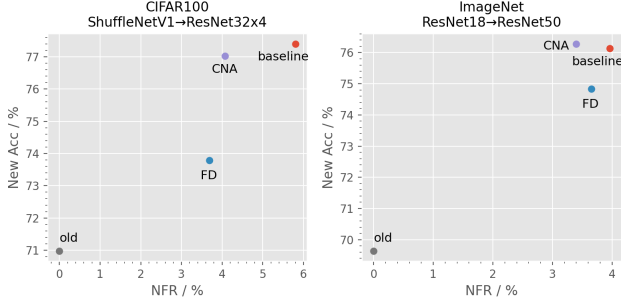


Figure 3. Results of model upgrade on CIFAR100 and ImageNet. X-axis: negative flips rate (NFR) in %, lower is better. Y-axis: new model accuracy in % higher is better. The idea model is expected to be located in the top-left corner.

4.2.1 Baselines

Knowledge Distillation was proposed in [16] to distill the knowledge from a pre-trained source (teacher) model to a newly trained target (student) model. It forces the target output probabilities to mimic those of the source, by minimizing a KL divergence loss between them,

$$\ell_{KD}(h_T(x_i), h_S(x_i)) = \tau^2 KL(h_T(x_i)/\tau, h_S(x_i)/\tau), \quad (10)$$

where $h(\cdot)$ is the classifier prediction, KL is KL divergence and τ is the temperature.

Local Feature Alignment: To address the issue that LLE [34] lacks the ability of generalizing to points unknown to training data, [13] proposed to learn a non-linear mapping to preserve the local neighborhood by contrastive learning. This idea can also be applied here to align the local feature representations, called *local feature alignment* (LFA). Given the feature representations of the source model $f_S(x_i)$ and the target model $f_T(x_j)$, the idea is to pull them together if x_i and x_j are the same sample, otherwise repel them. The loss is defined as:

$$\begin{aligned} \ell_{FA}(x_i, x_j) = & \mathbb{1}[i = j] \frac{1}{2} \|f_T(x_j) - f_S(x_i)\|_2^2 \\ & + \mathbb{1}[i \neq j] \frac{1}{2} [\max(0, \xi - \|f_T(x_j) - f_S(x_i)\|_2)]^2 \end{aligned} \quad (11)$$

where $\mathbb{1}[\cdot]$ is an indicator function and ξ is a margin hyperparameter in the hinge loss term. Similar to CNA loss of Eq. (5), local structure can be aligned by LFA, but the difference is LFA directly optimizes on the ℓ_2 feature distance.

Similar to Eq. (7), the KD loss of Eq. (10) and FA loss of Eq. (11) is jointly optimized with a cross-entropy loss with trade-off coefficient λ in the model distillation task.

4.2.2 Model distillation

We compare CNA to the KD and LFA baselines as introduced in Sec. 4.2.1, and the recent contrastive representa-

Table 4. Ablation studies on batch size.

batch size	32	64	128	256	512	1024
CIFAR100	71.51	71.36	71.87	71.79	71.96	-
ImageNet	-	-	70.75	70.87	71.08	71.38

tion distillation (CRD) [43]. We followed [43] for the experimental settings for model distillation. In detail, the models on CIFAR100 (ImageNet) were trained for 240 (100) epochs. Differently, we used cosine learning rate scheduling instead of a hand designed schedule. The default batch size is 1024 (512) for CNA and 512 for KD and LFA, on ImageNet (CIFAR100). We re-implemented the KD baseline following [16], but set loss trade-off $\lambda = 1$ and temperature $\tau = 100$, which yielded better results. For LFA, the margin $\xi = 3.0$ for all experiments, but we searched for the best trade-off λ since it is sensitive.

The results are shown in Tab. 2 for CIFAR100 and Tab. 3 for ImageNet. In the first part of Tab. 2, the target and source models are of the same architectural style, but of different styles in the second part. Besides KD [16], LFA and CRD [43], some recent works of SP [44], CC [32], VID [2] and RKD [31] are also compared. First, we found that our KD and LFA baselines already achieved very good results, better than SP, CC, VID and RKD in most of cases, and comparable to CRD. But the results of LFA are sometimes unreliable. For example, when distilling “ResNet32x4” to “ResNet8x4” on CIFAR100 or distilling “ResNet50” to “ResNet18” on ImageNet, LFA underperforms KD, CRD and CNA by a large margin. This is probably due to the direct optimization of LFA on the ℓ_2 feature distance. Next, our CNA achieved reliable results comparable to KD and CRD, although CNA only tries to preserve the local topology, irrespective of the representation knowledge as distilled by KD. This shows the effectiveness of the proposed CNA even when it is evaluated for a classification task. The observations are similar in the experiments of ImageNet in Tab. 3, showing that the CNA can generalize well on different datasets.

4.2.3 Reducing Regression in Model Upgrade

In [51] the problem of regression in model upgrade is introduced. A variant of KL-divergence based distillation loss was used to reduce the amount of new errors introduced by a new model in comparison to an old reference model. We expect the capacity of CNA in preserving the structure knowledge would also help reduce the regression. We compare CNA to (i) a naive baseline approach to train the new model using the standard cross-entropy loss - no attempt to address model regression is considered in this case (ii) the latest approach using focal distillation (FD) [51].

Metrics: We evaluated the negative flip rate (NFR) [51] and the accuracy for each model. The NFR is defined as the

Table 5. Ablation studies on Number of MLP.

# MLP	0	1	2
CIFAR100	71.96	71.56	71.49
ImageNet	71.38	71.01	71.00

fraction of negative flips:

$$\text{NFR} = \frac{1}{N} \sum_{i=1}^N \mathbb{1}[\hat{y}_n^{(i)} \neq y_i \text{ and } \hat{y}_o^{(i)} = y_i] \quad (12)$$

where $\hat{y}_n^{(i)}$ and $\hat{y}_o^{(i)}$ are the predicted labels of the new model and the old model for input image x_i , and N is the number of samples in the test set $\mathcal{S}_{test} = \{(x_i, y_i), i = 1..N\}$.

All models in these experiments were trained with batch size 512. On CIFAR100 (ImageNet), the model was trained for 240 (90) epochs, with learning rate decreased by 0.1 every 80 (30) epochs. For CNA, the trade-off λ in Eq. (7) is chosen by validation as 1 for CIFAR100 and 0.2 for ImageNet. To ensure a fair comparison, the hyper-parameters for focal distillation were also chosen through the same validation split of CNA.

We consider the common model update scenario: the new model architecture is larger than that of the old model. We evaluated a variety of architecture changes, including ShuffleNet and ResNet variants. The models were both trained on the same dataset. The results are visualized in Fig. 3. We observe that CNA can consistently reduce the NFR. In particular, the relative NFR reduction compared to the baseline new model is 29.9% on CIFAR100 and 14.1% on ImageNet. On ImageNet, CNA slightly improves the model accuracy from 76.13% to 76.28%. CNA outperforms focal distillation by obtaining higher accuracy with comparable or lower NFR. This performance improvement can be attributed to the benefits of imposing direct representation regularization instead of mimicking the input-output behavior via knowledge distillation. The latter in the scenario of model upgrade would cause inevitable accuracy degradation of the new model, which the CNA does not suffer from.

Table 6. Ablation studies on temperature.

temperature	0.001	0.01	0.05	0.1
CIFAR100	71.42	71.96	71.44	70.40
ImageNet	70.87	71.38	70.84	70.52

Table 7. Ablation studies on number of neighbors K .

K	1	2	4	8
CIFAR100	71.96	71.94	71.50	71.41
ImageNet	71.38	71.26	71.14	71.02

4.3. Ablation Studies

To further understand the performance of CNA, we conducted a series of model distillation ablation studies. The source/target model is ResNet56/ResNet20 on CIFAR100 and ResNet34/ResNet18 on ImageNet. The default settings are: temperature $\tau = 0.01$, number of neighbors $K = 1$, number of MLP is 0 and batch size is 512 (1024) for CIFAR100 (ImageNet).

Batch Size. The effect of batch size is investigated in Tab. 4. It can be found that the CNA algorithm is quite robust to different batch sizes on CIFAR100, as long as the batch size is not smaller than 128. But the performance decreases when the batch size becomes smaller on ImageNet. This is probably because there are 1,000 classes for ImageNet and it is possible there is no very close neighbor in a single batch if the batch size is too small. Relatively large batch size is preferred for CNA to better preserve the local structure.

Temperature τ was ablated in Tab. 6. It shows the best choice is around $\tau = 0.01$. When it is decreased or increased too much, the performances drop. This temperature is also robust to different datasets.

Number of neighbors K in Eq. (6) was ablated in Tab. 7. On both datasets, $K = 1$ performs considerably well, but the performances decrease when more neighbors were counted in the loss function of Eq. (6). This is probably because the contrastive loss formulation (Eq. (6)) is curated for single pair contrast. Directly including the other neighbors without considering their further structure information, e.g. neighbor ranking, from the old model may impose inaccurate neighborhood regulation on the new model, thus degrading the performance.

Number of MLPs. The hidden MLP layers have been shown to be very helpful for representation learning [6, 14]. Results from investigations of its effect on CNA are shown in Tab. 5. It shows that the hidden MLP layer does not help in CNA. The possible reason could be that the goal of CNA, maintaining the local data structure, is different from the representation learning [6, 14].

5. Conclusion

In this paper, we proposed a new method, contrastive neighborhood alignment (CNA), that preserves the local structure of feature spaces between models. The effectiveness of CNA is illustrated on three problems: manifold learning, where the topology of the original data is maintained in a low-dimensional space using an inductive model, model distillation, where a compact student is trained to mimic a larger one, and model upgrade, where the new model is more powerful than the old one. Existing methods in model distillation are primarily focused on matching the output predictions/logits for the pair of models in question whereas CNA is motivated differently by preserv-

ing the local neighborhood structures of the samples in the representation spaces. The instance-level contrastive loss in CNA is empirically shown to work harmoniously with the standard cross-entropy loss.

Limitations: The concept of aligning the local neighborhoods is intuitive but its performance gain in model distillation still has room to improve. Nonetheless, CNA provides a new means for preserving the integrity of the model by matching the feature manifold using a contrastive term that has not been previously explored.

Potential Negative Societal Impacts: CNA may accidentally transfer the bias in the source feature embedding [5] to the target model. As a result it may unintentionally amplify these biases when deploying the model. Selecting unbiased source model or applying debiasing algorithm to the learned new model can mitigate this negative effect.

References

- [1] <https://github.com/dkozlov/awesome-knowledge-distillation>. 1
- [2] Sungsoo Ahn, Shell Xu Hu, Andreas Damianou, Neil D Lawrence, and Zhenwen Dai. Variational information distillation for knowledge transfer. In *Proceedings of the IEEE/CVF Conference on Computer Vision and Pattern Recognition*, pages 9163–9171, 2019. 6, 7
- [3] Stanislaw Antol, Aishwarya Agrawal, Jiasen Lu, Margaret Mitchell, Dhruv Batra, C Lawrence Zitnick, and Devi Parikh. Vqa: Visual question answering. In *ICCV*, 2015. 2
- [4] Jimmy Lei Ba, Jamie Ryan Kiros, and Geoffrey E Hinton. Layer normalization. *arXiv:1607.06450*, 2016. 2
- [5] Tolga Bolukbasi, Kai-Wei Chang, James Zou, Venkatesh Saligrama, and Adam Kalai. Man is to computer programmer as woman is to homemaker? debiasing word embeddings. *arXiv preprint arXiv:1607.06520*, 2016. 9
- [6] Ting Chen, Simon Kornblith, Mohammad Norouzi, and Geoffrey Hinton. A simple framework for contrastive learning of visual representations. In *International conference on machine learning*, pages 1597–1607. PMLR, 2020. 2, 8
- [7] Yu Cheng, Duo Wang, Pan Zhou, and Tao Zhang. A survey of model compression and acceleration for deep neural networks. *arXiv preprint arXiv:1710.09282*, 2017. 1
- [8] Jason V Davis, Brian Kulis, Prateek Jain, Suvrit Sra, and Inderjit S Dhillon. Information-theoretic metric learning. In *Proceedings of the 24th international conference on Machine learning*, pages 209–216, 2007. 2
- [9] David L Donoho and Carrie Grimes. Hessian eigenmaps: Locally linear embedding techniques for high-dimensional data. *Proceedings of the National Academy of Sciences*, 100(10):5591–5596, 2003. 1, 2, 3, 5
- [10] John Duchi, Elad Hazan, and Yoram Singer. Adaptive sub-gradient methods for online learning and stochastic optimization. *Journal of machine learning research*, 12(7), 2011. 2
- [11] Priya Goyal, Piotr Dollár, Ross Girshick, Pieter Noordhuis, Lukasz Wesolowski, Aapo Kyrola, Andrew Tulloch, Yangqing Jia, and Kaiming He. Accurate, large mini-batch sgd: Training imagenet in 1 hour. *arXiv preprint arXiv:1706.02677*, 2017. 6
- [12] Raia Hadsell, Sumit Chopra, and Yann LeCun. Dimensionality reduction by learning an invariant mapping. In *2006 IEEE Computer Society Conference on Computer Vision and Pattern Recognition (CVPR'06)*, volume 2, pages 1735–1742. IEEE, 2006. 2
- [13] Raia Hadsell, Sumit Chopra, and Yann LeCun. Dimensionality reduction by learning an invariant mapping. In *2006 IEEE Computer Society Conference on Computer Vision and Pattern Recognition (CVPR'06)*, volume 2, pages 1735–1742. IEEE, 2006. 7
- [14] Kaiming He, Haoqi Fan, Yuxin Wu, Saining Xie, and Ross Girshick. Momentum contrast for unsupervised visual representation learning. In *Proceedings of the IEEE/CVF Conference on Computer Vision and Pattern Recognition*, pages 9729–9738, 2020. 2, 8
- [15] Kaiming He, Xiangyu Zhang, Shaoqing Ren, and Jian Sun. Deep residual learning for image recognition. In *Proceedings of the IEEE conference on computer vision and pattern recognition*, pages 770–778, 2016. 2, 6
- [16] Geoffrey Hinton, Oriol Vinyals, and Jeff Dean. Distilling the knowledge in a neural network. *NIPS Deep Learning and Representation Learning Workshop*, preprint *arXiv:1503.02531*, 2015. 1, 2, 4, 5, 6, 7
- [17] Elad Hoffer and Nir Ailon. Deep metric learning using triplet network. In *International workshop on similarity-based pattern recognition*, pages 84–92, 2015. 2
- [18] Andrew G Howard, Menglong Zhu, Bo Chen, Dmitry Kalenichenko, Weijun Wang, Tobias Weyand, Marco Andreetto, and Hartwig Adam. Mobilenets: Efficient convolutional neural networks for mobile vision applications. *arXiv preprint arXiv:1704.04861*, 2017. 2
- [19] Jie Hu, Li Shen, and Gang Sun. Squeeze-and-excitation networks. In *CVPR*, 2018. 2
- [20] Prannay Khosla, Piotr Teterwak, Chen Wang, Aaron Sarna, Yonglong Tian, Phillip Isola, Aaron Maschinot, Ce Liu, and Dilip Krishnan. Supervised contrastive learning. *Advances in Neural Information Processing Systems*, 2020. 2, 4
- [21] Diederik P Kingma and Jimmy Ba. Adam: A method for stochastic optimization. *arXiv preprint arXiv:1412.6980*, 2014. 5
- [22] Ranjay Krishna, Yuke Zhu, Oliver Groth, Justin Johnson, Kenji Hata, Joshua Kravitz, Stephanie Chen, Yannis Kalantidis, Li-Jia Li, David A Shamma, et al. Visual genome: Connecting language and vision using crowdsourced dense image annotations. *International journal of computer vision*, 123(1):32–73, 2017. 2
- [23] Alex Krizhevsky. Learning multiple layers of features from tiny images. Technical report, 2009. 6
- [24] Alex Krizhevsky, Ilya Sutskever, and Geoffrey E Hinton. Imagenet classification with deep convolutional neural networks. In *Advances in neural information processing systems*, 2012. 2
- [25] Hildegard Kuehne, Hueihan Jhuang, Estíbaliz Garrote, Tomaso Poggio, and Thomas Serre. Hmdb: a large video database for human motion recognition. In *ICCV*, 2011. 2

- [26] Brian Kulis et al. Metric learning: A survey. *Foundations and trends in machine learning*, 5(4):287–364, 2012. 2
- [27] Yann LeCun, Léon Bottou, Yoshua Bengio, and Patrick Haffner. Gradient-based learning applied to document recognition. *Proceedings of the IEEE*, 86(11):2278–2324, 1998. 6
- [28] Tsung-Yi Lin, Michael Maire, Serge Belongie, James Hays, Pietro Perona, Deva Ramanan, Piotr Dollár, and C Lawrence Zitnick. Microsoft coco: Common objects in context. In *ECCV*, 2014. 2
- [29] Ningning Ma, Xiangyu Zhang, Hai-Tao Zheng, and Jian Sun. Shufflenet v2: Practical guidelines for efficient cnn architecture design. In *Proceedings of the European conference on computer vision (ECCV)*, pages 116–131, 2018. 6
- [30] Aaron van den Oord, Yazhe Li, and Oriol Vinyals. Representation learning with contrastive predictive coding. *arXiv:1807.03748*, 2018. 2
- [31] Wonpyo Park, Dongju Kim, Yan Lu, and Minsu Cho. Relational knowledge distillation. In *Proceedings of the IEEE/CVF Conference on Computer Vision and Pattern Recognition*, pages 3967–3976, 2019. 6, 7
- [32] Baoyun Peng, Xiao Jin, Jiaheng Liu, Dongsheng Li, Yichao Wu, Yu Liu, Shunfeng Zhou, and Zhaoning Zhang. Correlation congruence for knowledge distillation. In *Proceedings of the IEEE/CVF International Conference on Computer Vision*, pages 5007–5016, 2019. 6, 7
- [33] Pranav Rajpurkar, Jian Zhang, Konstantin Lopyrev, and Percy Liang. Squad: 100, 000+ questions for machine comprehension of text. In *EMNLP*, 2016. 2
- [34] Sam T Roweis and Lawrence K Saul. Nonlinear dimensionality reduction by locally linear embedding. *science*, 290(5500):2323–2326, 2000. 1, 2, 3, 5, 7
- [35] Olga Russakovsky, Jia Deng, Hao Su, Jonathan Krause, Sanjeev Satheesh, Sean Ma, Zhiheng Huang, Andrej Karpathy, Aditya Khosla, Michael S. Bernstein, Alexander C. Berg, and Fei-Fei Li. Imagenet large scale visual recognition challenge. *Int. J. Comput. Vis.*, 115(3):211–252, 2015. 2, 6
- [36] Bharat Bhusan Sau and Vineeth N Balasubramanian. Deep model compression: Distilling knowledge from noisy teachers. *arXiv preprint arXiv:1610.09650*, 2016. 4
- [37] Florian Schroff, Dmitry Kalenichenko, and James Philbin. Facenet: A unified embedding for face recognition and clustering. In *Proceedings of the IEEE conference on computer vision and pattern recognition*, pages 815–823, 2015. 2
- [38] Yantao Shen, Yuanjun Xiong, Wei Xia, and Stefano Soatto. Towards backward-compatible representation learning. In *CVPR*, 2020. 2
- [39] Karen Simonyan and Andrew Zisserman. Very deep convolutional networks for large-scale image recognition. In *ICLR*, 2015. 2
- [40] Christian Szegedy, Wei Liu, Yangqing Jia, Pierre Sermanet, Scott Reed, Dragomir Anguelov, Dumitru Erhan, Vincent Vanhoucke, and Andrew Rabinovich. Going deeper with convolutions. In *CVPR*, 2015. 2
- [41] Yaniv Taigman, Ming Yang, Marc’Aurelio Ranzato, and Lior Wolf. Deepface: Closing the gap to human-level performance in face verification. In *Proceedings of the IEEE conference on computer vision and pattern recognition*, pages 1701–1708, 2014. 2
- [42] Joshua B Tenenbaum, Vin De Silva, and John C Langford. A global geometric framework for nonlinear dimensionality reduction. *science*, 290(5500):2319–2323, 2000. 1, 2, 3, 5
- [43] Yonglong Tian, Dilip Krishnan, and Phillip Isola. Contrastive representation distillation. In *International Conference on Learning Representations*, 2020. 2, 6, 7
- [44] Frederick Tung and Greg Mori. Similarity-preserving knowledge distillation. In *Proceedings of the IEEE/CVF International Conference on Computer Vision*, pages 1365–1374, 2019. 6, 7
- [45] Laurens Van Der Maaten, Eric Postma, Jaap Van den Herik, et al. Dimensionality reduction: a comparative. *J Mach Learn Res*, 10(66-71):13, 2009. 2, 3, 6
- [46] Ashish Vaswani, Noam Shazeer, Niki Parmar, Jakob Uszkoreit, Llion Jones, Aidan N Gomez, Lukasz Kaiser, and Illia Polosukhin. Attention is all you need. In *Advances in Neural Information Processing Systems*, 2017. 2
- [47] Lin Wang and Kuk-Jin Yoon. Knowledge distillation and student-teacher learning for visual intelligence: A review and new outlooks. *IEEE Transactions on Pattern Analysis and Machine Intelligence*, 2021. 1, 2
- [48] Kilian Q Weinberger, Fei Sha, and Lawrence K Saul. Learning a kernel matrix for nonlinear dimensionality reduction. In *Proceedings of the twenty-first international conference on Machine learning*, page 106, 2004. 2, 3, 5, 6
- [49] Zhirong Wu, Yuanjun Xiong, Stella X Yu, and Dahua Lin. Unsupervised feature learning via non-parametric instance discrimination. In *CVPR*, 2018. 2
- [50] Saining Xie, Ross Girshick, Piotr Dollár, Zhuowen Tu, and Kaiming He. Aggregated residual transformations for deep neural networks. In *CVPR*, 2017. 2
- [51] Sijie Yan, Yuanjun Xiong, Kaustav Kundu, Shuo Yang, Siqi Deng, Meng Wang, Wei Xia, and Stefano Soatto. Positive-congruent training: Towards regression-free model updates. *arXiv:2011.09161*, 2020. 1, 2, 4, 7
- [52] Liu Yang and Rong Jin. Distance metric learning: A comprehensive survey. *Michigan State University*, 2(2):4, 2006. 2
- [53] Xiangyu Zhang, Xinyu Zhou, Mengxiao Lin, and Jian Sun. Shufflenet: An extremely efficient convolutional neural network for mobile devices. In *Proceedings of the IEEE conference on computer vision and pattern recognition*, pages 6848–6856, 2018. 6